

DO-TH 2004/13
December 2004

Probing the Perturbative NLO Parton Evolution in the Small- x Region

M. Glück, C. Pisano, E. Reya

*Universität Dortmund, Institut für Physik,
D-44221 Dortmund, Germany*

Abstract

A dedicated test of the perturbative QCD NLO parton evolution in the very small- x region is performed. We find a perfect agreement with recent precision HERA-data for $F_2^p(x, Q^2)$, as well as for the expected curvature of F_2^p .

Parton distributions $f(x, Q^2)$, $f = q, \bar{q}, g$, underlie a Q^2 –evolution dictated by perturbative QCD at $Q^2 \gtrsim 1 \text{ GeV}^2$. It was recently stated [1] that the NLO perturbative QCD Q^2 –evolution disagrees with HERA data [2, 3] on $F_2^p(x, Q^2)$ in the small– x region, $x \lesssim 10^{-2}$. In view of the importance of this statement we perform here an independent study of this issue. In contrast to [1] we shall undertake this analysis in the standard framework where one sets up input distributions at some low Q_0^2 , here taken to be $Q_0^2 = 1.5 \text{ GeV}^2$, corresponding to the lowest Q^2 considered in [1], and adapting these distributions to the data considered. In the present case the data considered will be restricted to

$$1.5 \text{ GeV}^2 \leq Q^2 \leq 12 \text{ GeV}^2, \quad 3 \times 10^{-5} \lesssim x \lesssim 3 \times 10^{-3} \quad (1)$$

as in [1] and will be taken from the corresponding measured $F_2^p(x, Q^2)$ of the H1 collaboration [2]. The choice of these data is motivated by their higher precision as compared to corresponding data of the ZEUS collaboration [3], in particular in the very small– x region.

We shall choose two sets of input distributions based on the GRV98 parton distributions [4]. In the first set we shall adopt $u_v, d_v, s = \bar{s}$ and $\Delta \equiv \bar{d} - \bar{u}$ from GRV98 and modify $\bar{u} + \bar{d}$ and the gluon distribution in the small– x region to obtain an optimal fit to the H1 data [2] in the aforementioned kinematical region. We shall refer to this fit as the ‘best fit’. The second choice will be constrained to modify the GRV98 $\bar{u} + \bar{d}$ and g distributions in the small– x region as little as possible. We shall refer to this fit as GRV_{mod}. It will turn out that both input distributions are compatible with the data to practically the same extent, i.e. yielding comparable χ^2/dof . In view of these observations we do not agree with the conclusions of ref. [1], i.e. we do not confirm a disagreement between the NLO Q^2 –evolution of $f(x, Q^2)$ and the measured [2, 3] Q^2 –dependence of $F_2^p(x, Q^2)$.

The remaining flavor–singlet input distributions at $Q_0^2 = 1.5 \text{ GeV}^2$ to be adapted to

the recent small- x data are expressed as

$$xg(x, Q_0^2) = N_g x^{-a_g} (1 + A_g \sqrt{x} + 7.283x) (1 - x)^{4.759} \quad (2)$$

$$x(\bar{u} + \bar{d})(x, Q_0^2) = N_s x^{-a_s} (1 + A_s \sqrt{x} - 4.046x) (1 - x)^{4.225} \quad (3)$$

where the parameters relevant for the large x -region, $x > 10^{-3}$, which is of no relevance for the present small- x studies, are kept unchanged and are taken from, e.g. GRV98 [4]. The refitted relevant small- x parameters turn out to be

$$\begin{aligned} \text{'best fit'} : \quad & N_g = 1.70, \quad a_g = 0.027, \quad A_g = -1.034 \\ & N_s = 0.171, \quad a_s = 0.177, \quad A_s = 2.613 \end{aligned} \quad (4)$$

$$\begin{aligned} \text{GRV}_{\text{mod}} : \quad & N_g = 1.443, \quad a_g = 0.125, \quad A_g = -2.656 \\ & N_s = 0.270, \quad a_s = 0.117, \quad A_s = 1.70 \end{aligned} \quad (5)$$

to be compared with the original GRV98 parameters [4]: $N_g = 1.443$, $a_g = 0.147$, $A_g = -2.656$ and $N_s = 0.273$, $a_s = 0.121$, $A_s = 1.80$. The resulting predictions are compared to the H1-data [2] in Fig. 1. These results are also consistent with the ZEUS-data [3] with partly lower statistics. The corresponding χ^2/dof are 0.50 for the ‘best fit’ ($dof = 48$) and 0.94 for GRV_{mod} ($dof = 50$), respectively. Our treatment of the heavy flavor contributions to F_2 differs from that in [1]. We evaluate these contributions in the fixed flavor $f = 3$ scheme of [4], together with the massive heavy quark (c, b) contributions, rather than in the $f = 4$ (massless) scheme utilized in [1]. We have checked, however, that our disagreement with [1] does not result from our $f = 3$ plus heavy quarks vs. the $f = 4$ massless quark calculations in [1]: we have also performed a fit for $f = 4$ massless quarks and the results for F_2 and its curvature, to be discussed below, remain essentially unchanged. We are thus unable to trace the origin of our disagreement with the results and conclusion reached in [1].

In Figs. 2 and 3 we show our gluon and sea input distributions in (2) and (3), as well as their evolved shapes at $Q^2 = 4.5 \text{ GeV}^2$ in the small- x region. It can be seen that both

of our new small- x gluon distributions at $Q^2 = 4.5 \text{ GeV}^2$ conform to the rising shape obtained in most available analyses published so far, in contrast to the valence-like shape obtained in [1] where the gluon density xg decreases as $x \rightarrow 0$. It is possible to conceive a valence-like gluon at some very-low Q^2 scale, as in [4], but even in this extreme case the gluon ends up as non valence-like at $Q^2 > 1 \text{ GeV}^2$, in particular at $Q^2 = 4.5 \text{ GeV}^2$, as physically expected.

Turning now to the curvature test of F_2 advocated and discussed in [1], we first present in Fig. 4 our results for $F_2(x, Q^2)$ at $x = 10^{-4}$, together with two representative expectations of global fits [5, 6], as a function of [1]

$$q = \log_{10} \left(1 + \frac{Q^2}{0.5 \text{ GeV}^2} \right). \quad (6)$$

This variable has the advantage that most measurements lie along a straight line [1] as indicated by the dotted line at $x = 10^{-4}$ in Fig. 4. The MRST01 parametrization [5] results in a sizable curvature for F_2 in contrast to all other fits shown in Fig. 4. This large curvature is mainly caused by the valence-like input gluon distribution of MRST01 at $Q_0^2 = 1 \text{ GeV}^2$ in the small- x region which becomes even negative for $x < 10^{-3}$ [5]. More explicitly the curvature can be directly extracted from

$$F_2(x, Q^2) = a_0(x) + a_1(x)q + a_2(x)q^2. \quad (7)$$

The curvature $a_2(x) = \frac{1}{2} \partial_q^2 F_2(x, Q^2)$ is evaluated by fitting the predictions for $F_2(x, Q^2)$ at fixed values of x to a (kinematically) given interval of q . In Fig. 5(a) we present $a_2(x)$ which results from experimentally selected q -intervals [1]:

$$\begin{aligned} 0.7 \leq q \leq 1.4 & \text{ for } x = 4 \times 10^{-3}, \quad 1 \times 10^{-3}, \quad 3.2 \times 10^{-4} \\ 0.7 \leq q \leq 1.2 & \text{ for } x = 1.3 \times 10^{-4} \\ 0.6 \leq q \leq 0.8 & \text{ for } x = 5 \times 10^{-5}. \end{aligned} \quad (8)$$

Notice that the average value of q decreases with decreasing x due to the kinematically more restricted Q^2 range accessible experimentally. For comparison we show in Fig. 5(b)

the curvature $a_2(x)$ for an x –independent fixed q –interval

$$0.6 \leq q \leq 1.4 \quad (1.5 \text{ GeV}^2 \leq Q^2 \leq 12 \text{ GeV}^2). \quad (9)$$

Apart from the rather large values of $a_2(x)$ specific for the MRST01 fit as discussed above, our ‘best fit’ and GRV_{mod} results, based on the inputs in (4) and (5), respectively, do perfectly agree with the experimental curvatures as calculated and presented in [1].

To conclude, the perturbative NLO evolution of parton distributions in the small– x region is perfectly compatible with recent high–statistics measurements of the Q^2 –dependence of $F_2^p(x, Q^2)$ in that region. This is in contrast to the conclusions reached in [1].

This work has been supported in part by the ‘Bundesministerium für Bildung und Forschung’, Berlin/Bonn.

References

- [1] D. Haidt, *Eur. Phys. J.* **C35**, 519 (2004)
- [2] C. Adloff et al., H1 Collab., *Eur. Phys. J.* **C21**, 33 (2001)
- [3] S. Chekanov et al., ZEUS Collab., *Eur. Phys. J.* **C21**, 443 (2001)
- [4] M. Glück, E. Reya, A. Vogt, *Eur. Phys. J.* **C5**, 461 (1998)
- [5] A.D. Martin, R.G. Roberts, W.J. Stirling, R.S. Thorne, *Eur. Phys. J.* **C23**, 73 (2002)
- [6] J. Pumplin et al., *JHEP* **7**, 12 (2002) [hep–ph/0201195]

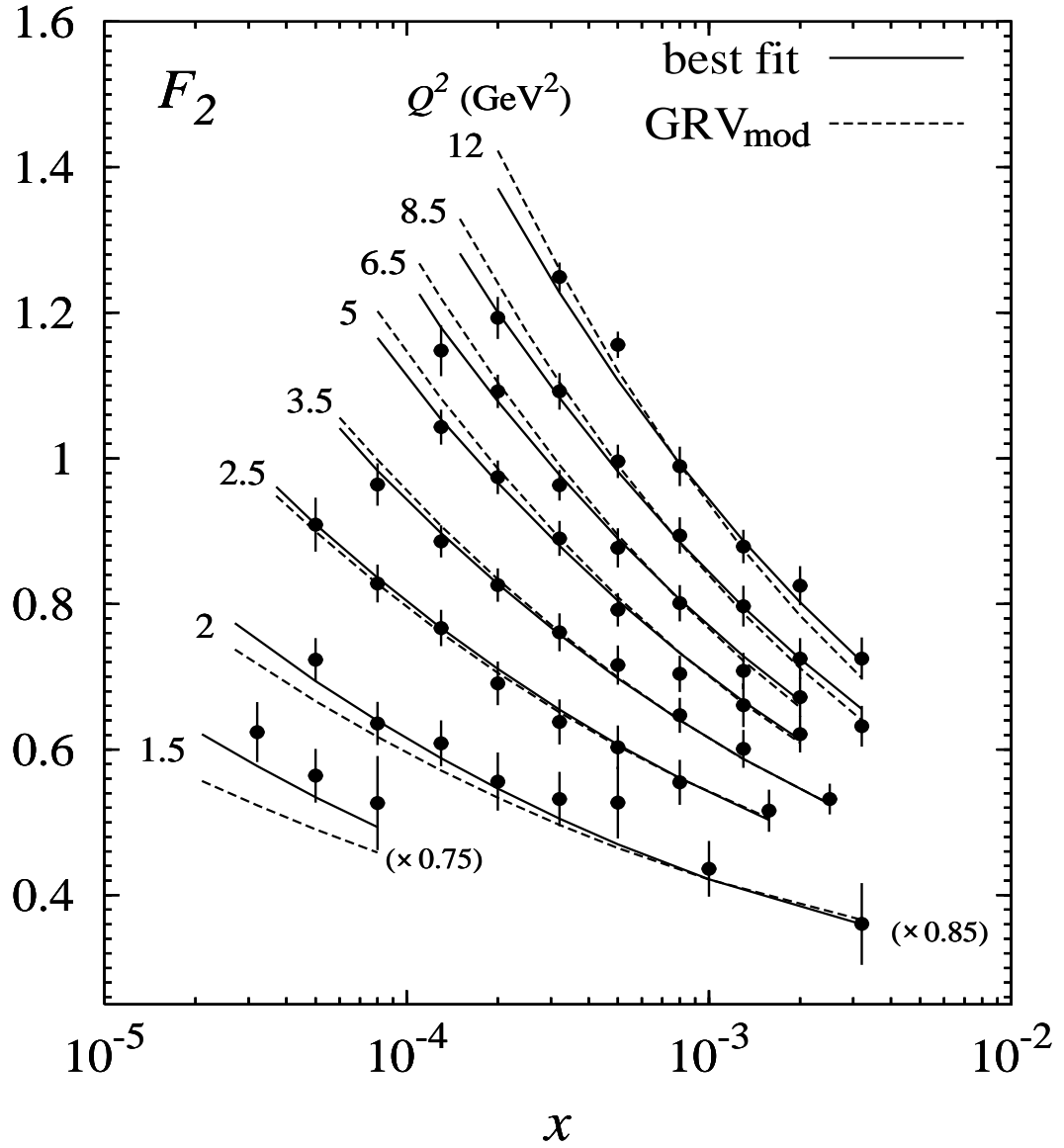


Figure 1: Comparison of our ‘best fit’ and GRV_{mod} results based on (4) and (5), respectively, with the H1 data [2]. To ease the graphical representation, the results and data for the lowest bins in $Q^2 = 1.5 \text{ GeV}^2$ and 2 GeV^2 have been multiplied by 0.75 and 0.85, respectively, as indicated

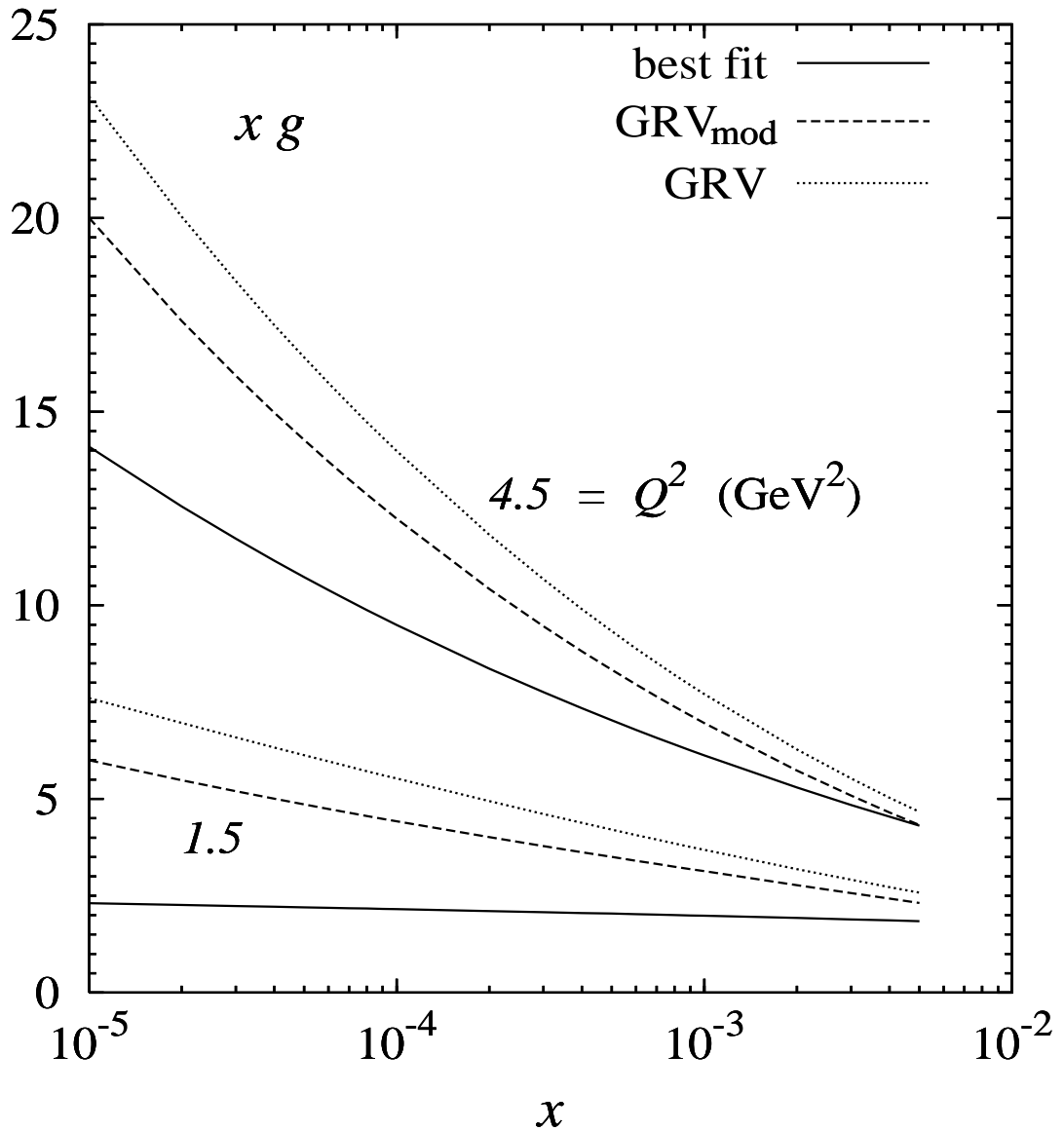


Figure 2: The gluon distributions at the input scale $Q_0^2 = 1.5 \text{ GeV}^2$ corresponding to (2) with the ‘best fit’ and GRV_{mod} parameters in (4) and (5), respectively, and at $Q^2 = 4.5 \text{ GeV}^2$. For comparison, the original GRV98 results [4] are shown as well by the dotted curves

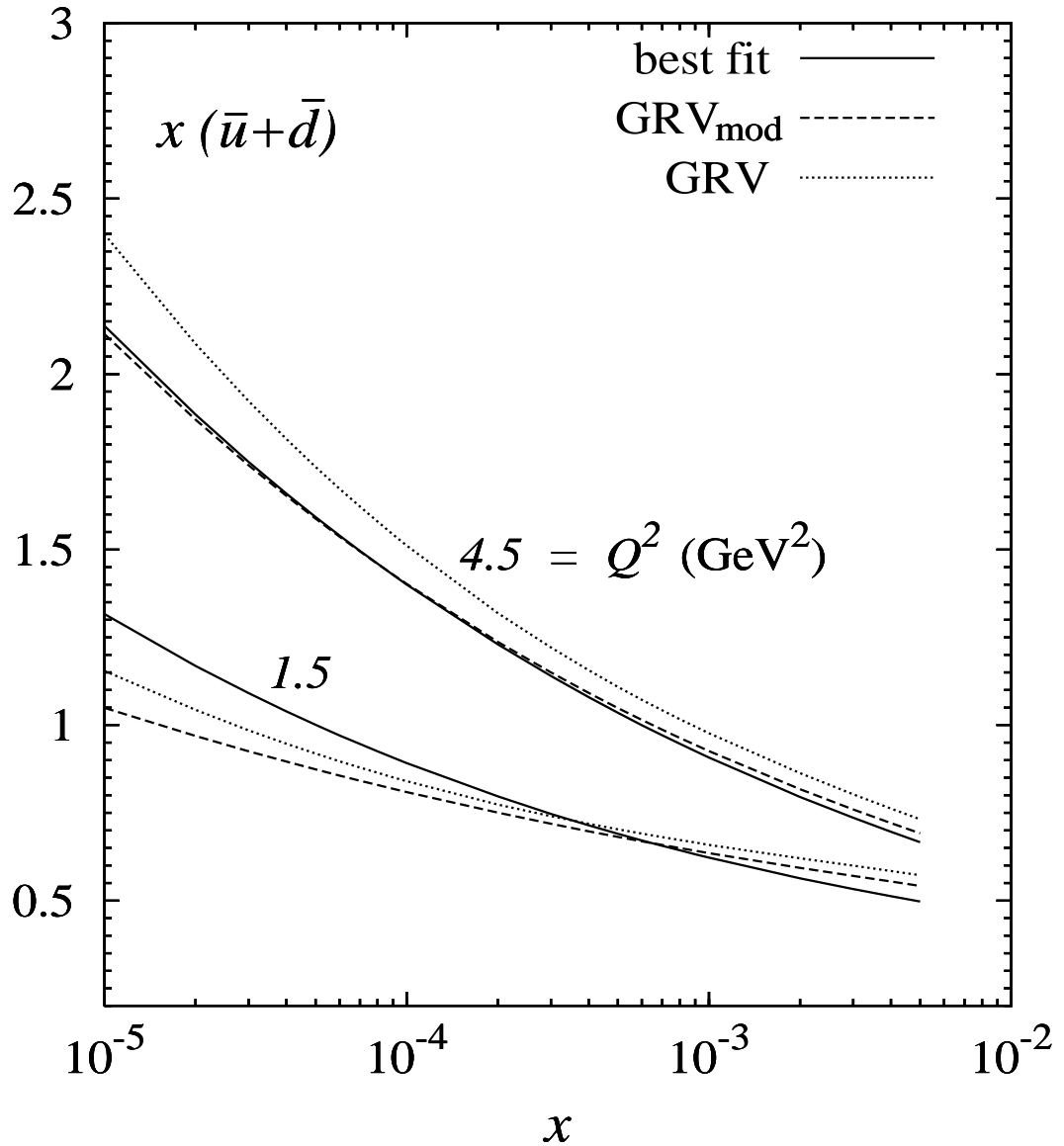


Figure 3: The sea distribution $x(\bar{u} + \bar{d})$ at the input scale $Q_0^2 = 1.5 \text{ GeV}^2$ in (3) with the ‘best fit’ and GRV_{mod} parameters in (4) and (5), respectively, and at $Q^2 = 4.5 \text{ GeV}^2$. For comparison, the original GRV98 results [4] are shown as well by the dotted curves

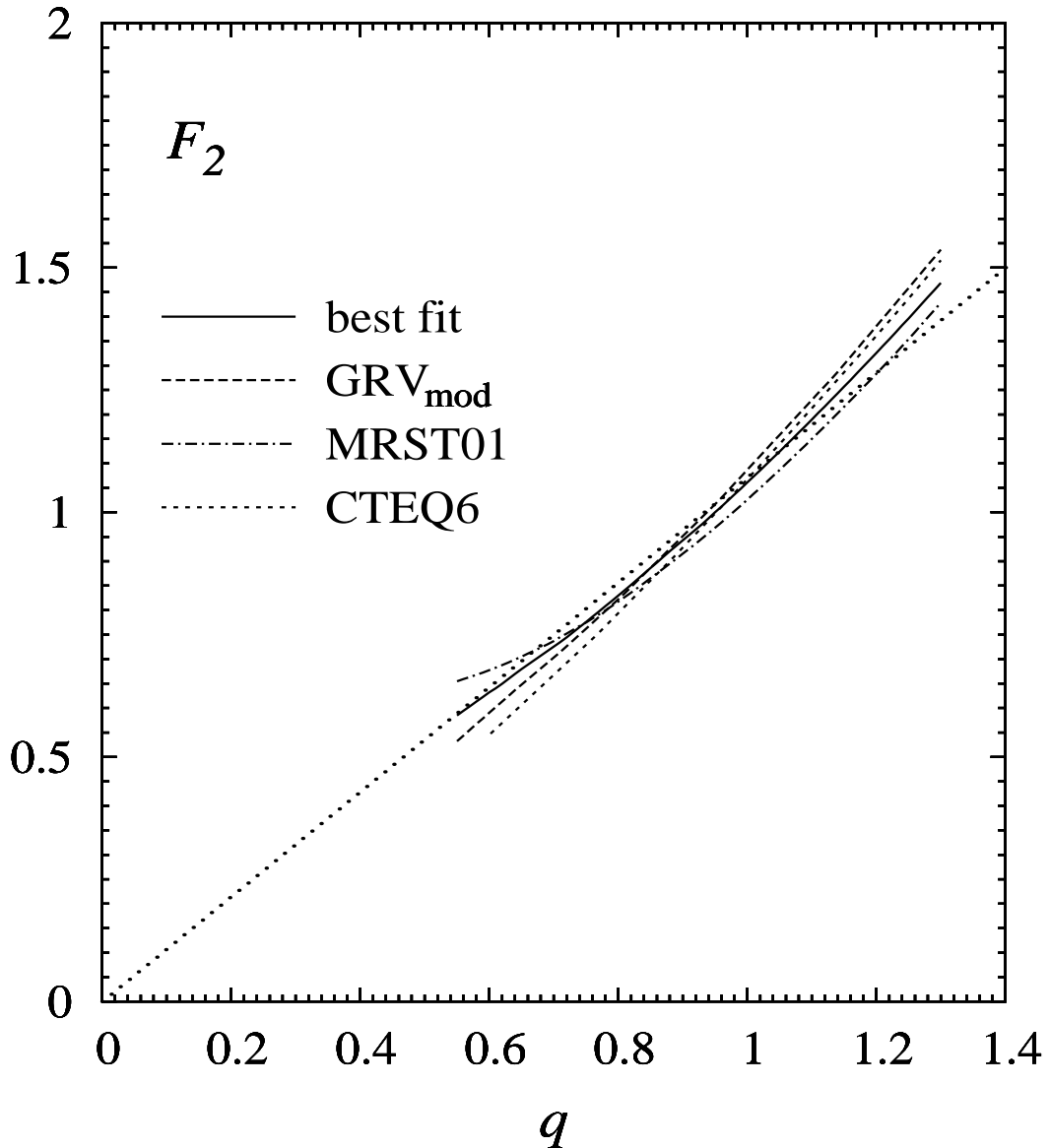


Figure 4: Predictions for $F_2(x, Q^2)$ at $x = 10^{-4}$ plotted versus q defined in (6). Representative global fit results are taken from MRST01 [5] and CTEQ6M [6]. Most small- x measurements lie along the straight (dotted) line [1]

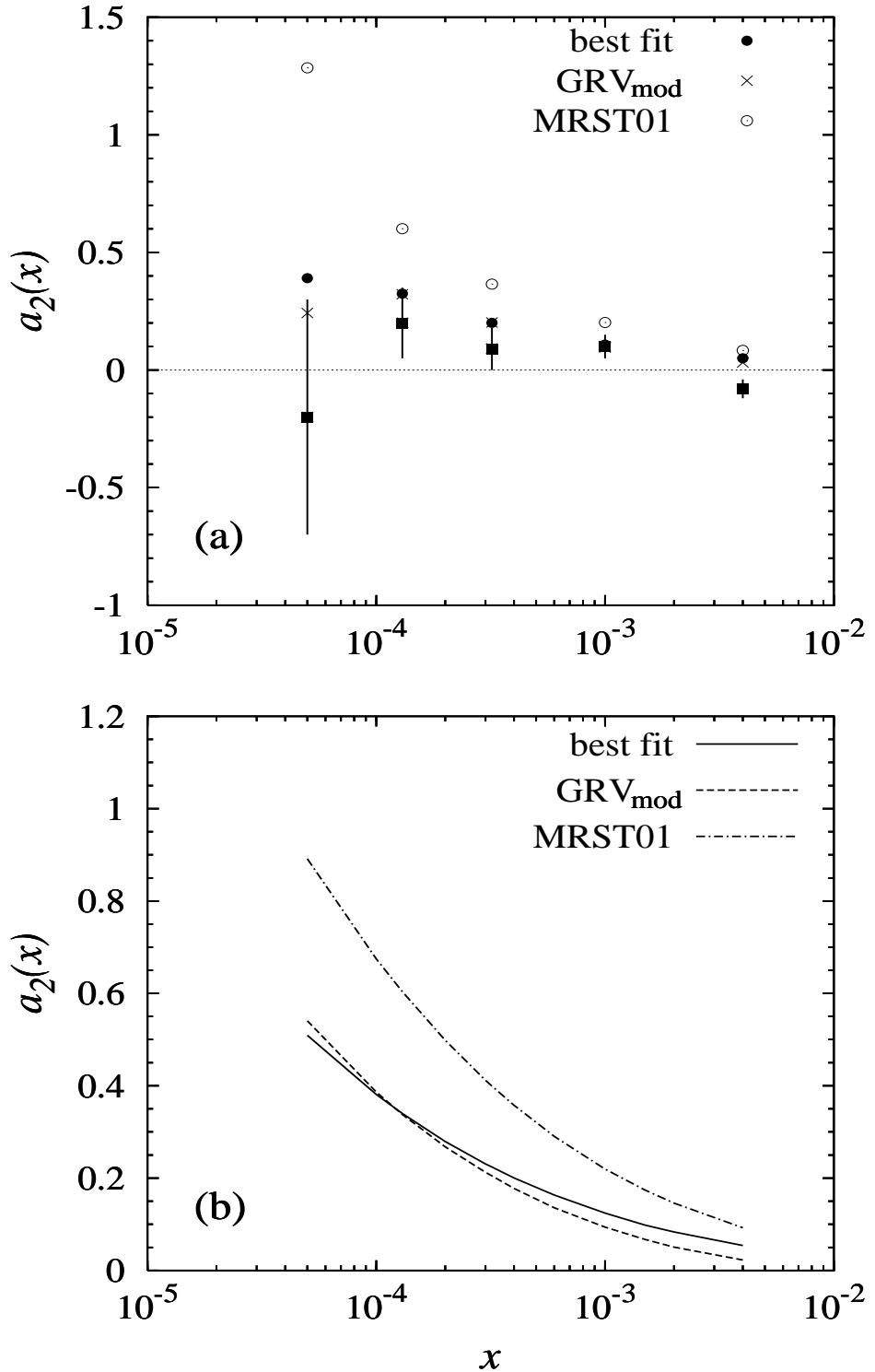


Figure 5: The curvature $a_2(x)$ as defined in (7) for (a) the variable q -intervals in (8) and (b) the fixed q -interval in (9). Also shown are the corresponding MRST01 results [5]. The experimental curvatures (squares) shown in (a) are taken from [1]